Smart Structures and Systems, *Vol. 25, No. 4 (2020) 393-399*
DOI: https://doi.org/10.12989/sss.2020.25.4.393

Design method for the 2DOF electromagnetic vibrational energy harvester

Shi-Baek Park [1a] and Seon-Jun Jang [*2]

[1] *Department of Mechanical Engineering, Yonsei University, Seoul, 03722, Republic of Korea*
[2] *School of Mechanical Engineering, Hoseo University, Asan 31499, Republic of Korea*

(*Received May 17, 2019, Revised July 31, 2019, Accepted July 31, 2019*)

Abstract. In this paper, the design method and experimental validation for the two-degree-of-freedom (2DOF) electromagnetic energy harvester are presented. The harvester consists of the rigid body suspended by four tension springs and electromagnetic transducers. Once the two resonant frequencies and the mass properties are specified, both the constant and the positions for the springs can be determined in the closed form. The designed harvester can locate two resonant peaks close to each other and forms the extended frequency bandwidth for power harvesting. Halbach magnet array is also introduced to enhance the output power. In the experiment, two resonant frequencies are measured at 34.9 and 37.6 Hz and the frequency bandwidth improves to 5 Hz at the voltage level of 207.9 mV. The normalized peak power of 4.587 mW/G^2 is obtained at the optimal load resistor of 367 Ω.

Keywords: vibration; energy harvester; resonant frequency; bandwidth; electromagnetic transducer; Halbach array

1. Introduction

Vibration energy harvesting harnesses the kinetic energy from the surrounding environment. It is one of the vital technology for future battery-less sensors. Recently, the vibration energy harvesters with electromagnetic transducers have been actively investigated (Ashraf *et al.* 2013, Nico *et al.* 2016, Nammari *et al.* 2018). Especially in civil engineering applications, many researches on the energy harvesting have been reported (Makihara *et al.* 2015, Kim *et al.* 2016, and Marian and Giaralis 2017). Since they usually utilized the resonance of the embedded spring-mass system, the slight detuning may result in a drastic drop in the generated power output (Zhu *et al.* 2010). Thus, the intensive researches have been carried out to make the vibration energy harvester robust in the variation of the exciting frequency. Ramlan *et al.* (2010) and Tang and Yang (2012) took advantage of the nonlinear vibrating system in increasing the bandwidth of the power output. Shahruz (2006), Ferrari *et al*. (2008), and Marin *et al.* (2013) proposed a parallel set of multiple single degree-of-freedom (DOF) harvesters whose natural frequencies were uniformly distributed over the bandwidth. Wu *et al.* (2014) and O'Donoghue *et al.* (2018) developed a 2DOF harvester where two single DOF spring-mass systems were serially connected. Wang and Tang (2017) studied a bistable 2DOF piezoelectric energy harvester with magnetic coupling in which a linear parasitic oscillator attached to the primary energy harvesting beam was used to generate two resonant peaks. Wong *et al.* (2009) designed a 3DOF harvester using a three mass-spring-damper chain system. Zhang *et al.* (2016) tested a broadband electrostatic energy harvester with a dual resonance structure consisting of two cantilever-mass subsystems, each with a mass attached at the free edge of a cantilever. Chen and Wu (2016) fabricated a 2DOF vibration structure formed by integrating a spiral diaphragm into a U-shaped cantilever to increase the usable bandwidth of a micromachined electromagnetic energy harvester. These researches utilized the multiple modes of multiple spring-mass systems connected in parallel or serial to improve the harvesting bandwidth. Meanwhile, Liu *et al.* (2012) fabricated a 3DOF electromagnetic MEMS energy harvester in which an elastically suspended single mass vibrates at three directional excitations of different frequencies. Their work distinguishes from previous by using the multiple DOF of the vibrating system of a single mass. Jang *et al.* (2010) and Kim *et al.* (2011) introduced a piezoelectric cantilever type energy harvester which utilized the vertical translation and rotation (2DOF) of a single proof mass. They connected two natural frequencies of a vibration system by placing them close together and achieved an enhanced bandwidth. Their harvester also utilized a single proof mass and can work at the unidirectional excitation.

In this work, a 2DOF electromagnetic energy harvester of the single proof mass working at the unidirectional excitation is proposed. The motion of the spatial mass is constrained into the vertical translation and rotation (2DOF) by using four vertical tension springs. Halbach magnet array is introduced to increase the output power. We derived the analytic design equations, which can be utilized in finding the positions and the constant of springs satisfying two target resonant frequencies. The frequency bandwidth for power harvesting can be enhanced by locating two resonant frequencies close to each other. The prototype

*Corresponding author, Ph.D., Assistant Professor,
E-mail: mweagle@hoseo.edu
[a] Ph.D.

Copyright © 2020 Techno-Press, Ltd.
http://www.techno-press.org/?journal=sss&subpage=7
ISSN: 1738-1584 (Print), 1738-1991 (Online)

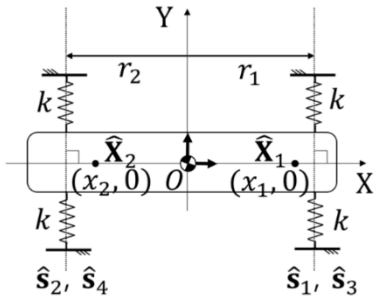

Fig. 1 Schematic of the 2DOF vibrating system in a plane

realization was conducted to verify the proposed design equations.

2. Analyses on the 2DOF vibrating system

2.1 Free vibration analysis

Fig. 1 shows a vibrating system which is composed of a rigid bar and four springs. The rigid bar plays a role of a proof mass, and four springs are installed parallel to the *Y*-axis. The springs have the same stiffness constant and are pretensioned that the motion of the rigid bar is confined to the 2DOF, i.e., rotation on the *X*-*Y* plane and translation in the *Y*- axis. In this paper, the Plücker's line coordinates are utilized in describing the model for the geometrical analysis of the multi-DOF vibrating system (Blanchet 1988). The Jacobian matrix containing the line vectors of the four springs expressed in Plücker's ray coordinates can be given by

$$\mathbf{j} = [\hat{\mathbf{s}}_1, \cdots, \hat{\mathbf{s}}_4] = \begin{bmatrix} 0 & 0 & 0 & 0 \\ 1 & 1 & 1 & 1 \\ r_1 & r_1 & -r_2 & -r_2 \end{bmatrix} \tag{1}$$

where r_i is the distance from the mass center to the *i*-th spring and $i = 1{,}2$. The stiffness matrix can be determined by (Griffis and Duffy 1991)

$$\mathbf{K} = k\mathbf{j}\mathbf{j}^T = \begin{bmatrix} 0 & 0 & 0 \\ 0 & 4k & 2k(r_1 - r_2) \\ 0 & 2k(r_1 - r_2) & 2k({r_1}^2 + {r_2}^2) \end{bmatrix} \tag{2}$$

The mass matrix of the rigid body at the mass center, *O* can be expressed by

$$\mathbf{M} = \mathrm{diag}(m, m, J) \tag{3}$$

where *m* is the mass of the rigid bar and *J* is the mass moment of inertia. When the harmonic motion is assumed, the infinitesimal displacement of the rigid bar can be expressed 2as

$$\mathbf{X} = \hat{\mathbf{X}}\mathrm{e}^{j\Omega t} \tag{4}$$

where $\hat{\mathbf{X}} = [\delta x, \delta y, \phi]^T$. δx, δy, and ϕ are respectively the *X*-, *Y*- translation, and the *Z*- rotation. The equation of motion for the free vibration of the vibrating system with the mass and stiffness matrices of Eqs. (2) and (3) can be expressed by

$$(\mathbf{K} - \Omega_i^2\mathbf{M})\hat{\mathbf{X}}_i = 0 \tag{5}$$

where Ω_i is the resonant frequency of the *i*-th mode, and $\hat{\mathbf{X}}_i$ is the corresponding vibration mode vector. $\hat{\mathbf{X}}_i$ can be normalized by the rotation ϕ_i and rewritten as

$$\hat{\mathbf{X}}_i = [y_i \quad -x_i \quad 1]^T \tag{6}$$

where $x_i \equiv -\frac{\delta y_i}{\phi_i}$ and $y_i \equiv \frac{\delta x_i}{\phi_i}$. The mode vector of Eq. (6) is the Plücker's axis coordinates of line perpendicular to the *X*-*Y* plane and passing through $(x_i,\ y_i)$. It can be geometrically interpreted as the small repetitive rotation about the vibration center of *i*-th mode, $(x_i,\ y_i)$. In the present study, since the stiffness matrix of Eq. (2) is singular and corresponds only to *Y*- translation and rotation on the *X*-*Y* plane, there exist two mode vectors found as

$$\hat{\mathbf{X}}_1 = [0 \quad -x_1 \quad 1]^T \tag{7a}$$

$$\hat{\mathbf{X}}_2 = [0 \quad -x_2 \quad 1]^T \tag{7b}$$

which can be interpreted as the vibration centers are lying on the *X*- axis at $(x_1,\ 0)$ and $(x_2,\ 0)$, respectively, as shown in Fig. 1.

Introducing the orthogonality condition of modes concerning the mass matrix gives (Meirovitch 2001)

$$\hat{\mathbf{X}}_1^T\mathbf{M}\hat{\mathbf{X}}_2 = mx_1x_2 + J = 0 \tag{8}$$

Eq. (8) can be satisfied only if the signs of x_1 and x_2 are different. Rewriting x_2 in terms of x_1 yields

$$x_2 = -\frac{J}{m}\frac{1}{x_1} = -\alpha^2\frac{1}{x_1} \tag{9}$$

where $\alpha = \sqrt{J/m}$ is radius of gyration.

2.2 Base excited vibration analysis

When the elastically supported rigid body is subject to a harmonic base excitation as shown in Fig. 2, the equation of motion of the body can be expressed by

$$\mathbf{M}\ddot{\mathbf{Z}} + \mathbf{C}\dot{\mathbf{Z}} + \mathbf{K}\mathbf{Z} = -\mathbf{M}\ddot{\mathbf{X}}_\mathbf{0} \tag{10}$$

where **C** is damping matrix, **Z** is relative displacement of the rigid body, i.e., $\mathbf{Z} = \mathbf{X} - \mathbf{X_0}$. Applying Eq. (4), $\mathbf{Z} = \hat{\mathbf{Z}}\mathrm{e}^{j\Omega t}$, and $\mathbf{X_0} = \hat{\mathbf{X}}_0\mathrm{e}^{j\Omega t}$to Eq. (10) yields

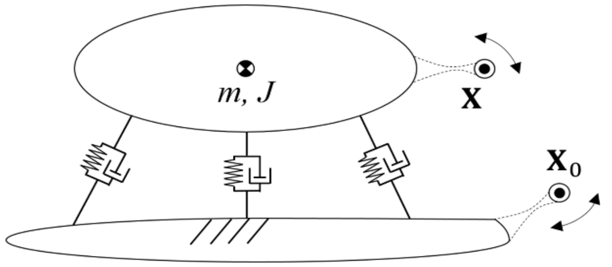

Fig. 2 Base excitation system

$$(\mathbf{K} - \Omega^2\mathbf{M} + j\Omega\mathbf{C})\hat{\mathbf{Z}} = \Omega^2\mathbf{M}\hat{\mathbf{X}}_0 \tag{11}$$

In Eq. (11), Ω is the excitation frequency and $\hat{\mathbf{X}}_0$ is the line expressing the infinitesimal base excitation. The right side of Eq. (11) is the inertial force due to base excitation and can be expressed here as

$$\hat{\mathbf{w}} = \Omega^2\mathbf{M}\hat{\mathbf{X}}_0 \tag{12}$$

Recalling that $\hat{\mathbf{X}}_i$ are the mode vectors, the modal matrix is given by

$$\mathbf{S} = [\hat{\mathbf{X}}_1 \quad \hat{\mathbf{X}}_2 \quad \hat{\mathbf{X}}_3] \tag{13}$$

Then mass, stiffness, and damping matrices **M**, **K**, and **C** can be diagonalized by the modal matrix as

$$\mathbf{S}^T\mathbf{M}\mathbf{S} = \mathrm{diag}(\tilde{m}_1, \tilde{m}_2, \tilde{m}_3) \tag{14a}$$

$$\mathbf{S}^T\mathbf{K}\mathbf{S} = \mathrm{diag}(\tilde{k}_1, \tilde{k}_2, \tilde{k}_3) \tag{14b}$$

$$\mathbf{S}^T\mathbf{C}\mathbf{S} = \mathrm{diag}(\tilde{c}_1, \tilde{c}_2, \tilde{c}_3) \tag{14c}$$

It is noted here that the damping matrix **C** is assumed proportional to both the mass and the stiffness matrices. Applying Eq. (14) to Eq. (11) and rearranging gives the relative small displacement of the rigid body $\hat{\mathbf{Z}}$ as the linear combination of the mode vectors by

$$\hat{\mathbf{Z}} = \sum_{i=1}^{3} \frac{\hat{\mathbf{X}}_i^T\hat{\mathbf{w}}}{\left(\tilde{k}_i - \Omega^2\tilde{m}_i\right) + j\Omega\tilde{c}_i}\hat{\mathbf{X}}_i \tag{15}$$

If the i-th modal damping ratio ζ_i defined as $\zeta_i = \frac{\tilde{c}_i}{2\tilde{m}_i\Omega_i}$ are assumed to be small, i.e., $\zeta_i < 0.05$, the damped resonant frequencies are almost identical to the undamped resonant frequencies. Thus, when $\Omega = \Omega_i$ at resonance, the response at i-th resonant peak can be approximated as

$$\hat{\mathbf{Z}}_i \cong \frac{\hat{\mathbf{X}}_i^T\hat{\mathbf{w}}}{j\Omega_i\tilde{c}_i}\hat{\mathbf{X}}_i \tag{16}$$

The work done by a vibrating body under the inertial force $\hat{\mathbf{w}}$ at the i-th resonant frequency can be expressed as

$$W_i = \hat{\mathbf{w}}^T\hat{\mathbf{Z}}_i \tag{17}$$

As to the present 2DOF vibrating system of Fig. 1, the base motion is always applied along the Y-axis and the inertial force can be described as

$$\hat{\mathbf{w}} = \Omega^2\mathbf{M}[0 \quad a_{cc}/\Omega^2 \quad 0]^T \tag{18}$$

where a_{cc} is the dose of the acceleration. Further, the modal matrix of the present system has two vectors of Eq. (7) and one vector for the rigid body mode, i.e., the corresponding resonant frequency is zero, can be described as

$$\mathbf{S} = [\hat{\mathbf{X}}_1 \quad \hat{\mathbf{X}}_2 \quad \hat{\mathbf{X}}_3] = \begin{bmatrix} 0 & 0 & 1 \\ -x_1 & -x_2 & 0 \\ 1 & 1 & 0 \end{bmatrix} \tag{19}$$

Then the modal mass parameters can be expressed from Eqs. (3) and (19) by

$$\tilde{m}_i = \hat{\mathbf{X}}_i^T\mathbf{M}\hat{\mathbf{X}}_i = m(x_i^2 + \alpha^2) \tag{20}$$

where i = 1, 2. Substituting $\tilde{c}_i = 2\tilde{m}_i\Omega_i\zeta_i$ and Eqs. (18) and (20) into Eq. (17) yields the works at resonances as

$$W_i = \frac{ma_{cc}^2x_i^2}{j2\Omega_i^2(x_i^2 + \alpha^2)\zeta_i} \tag{21}$$

3. Design method

3.1 Derivation of the design equations

It is desirable that the proposed harvester produces the identical works at its two resonances. Assuming $\zeta_1 = \zeta_2$, substituting Eq. (9) to Eq. (21) and applying identical condition of $W_1 = W_2$ yields

$$x_1 = \pm\frac{\Omega_1}{\Omega_2}\alpha \tag{22}$$

The other location, x_2 can be found from Eq. (9) as

$$x_2 = \mp\frac{\Omega_2}{\Omega_1}\alpha \tag{23}$$

Eqs. (22) and (23) shows that the positions of the vibration centers can be determined from the specified target frequencies and the radius of gyration.

From Eq. (5), the equation for the stiffness matrix can be expressed by

$$\mathbf{K} = \mathbf{M}\mathbf{S}\mathbf{\Lambda}\mathbf{S}^{-1} \tag{24}$$

where $\mathbf{\Lambda} = \begin{bmatrix} \Omega_1^2 & 0 & 0 \\ 0 & \Omega_2^2 & 0 \\ 0 & 0 & 0 \end{bmatrix}$. Substituting Eqs. (3), (19), (22), and (23) into Eq. (24) yields

$$\mathbf{K} = \begin{bmatrix} 0 & 0 & 0 \\ 0 & \dfrac{m(\Omega_1^4 + \Omega_2^4)}{\Omega_1^2 + \Omega_2^2} & \dfrac{m\alpha\Omega_1\Omega_2(\Omega_2^2 - \Omega_1^2)}{\Omega_1^2 + \Omega_2^2} \\ 0 & \dfrac{m\alpha\Omega_1\Omega_2(\Omega_2^2 - \Omega_1^2)}{\Omega_1^2 + \Omega_2^2} & \dfrac{m\alpha^2\Omega_1^2\Omega_2^2}{\Omega_1^2 + \Omega_2^2} \end{bmatrix} \tag{25}$$

Equating Eq. (24) with Eq. (2) gives the spring constant and the locations of the springs as follows

$$k = \frac{m(\Omega_1^4 + \Omega_2^4)}{4(\Omega_1^2 + \Omega_2^2)} \tag{26}$$

$$\mathrm{r}_1 = 2\alpha \cdot \frac{\Omega_1\Omega_2^3}{\Omega_1^4 + \Omega_2^4} \tag{27a}$$

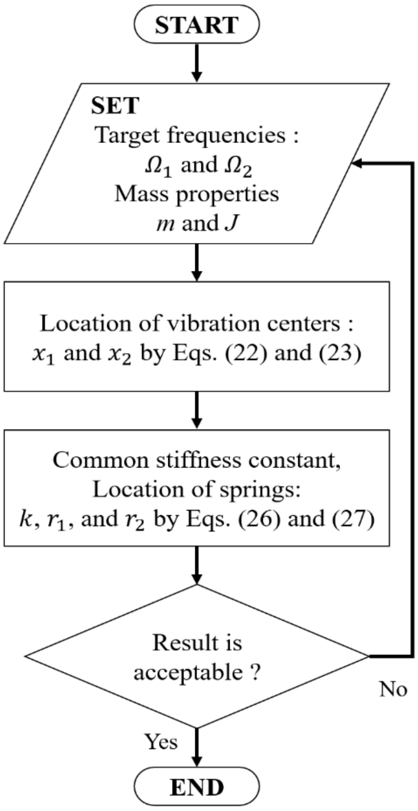

Fig. 3 Design procedure

$$r_2 = 2\alpha \cdot \frac{\Omega_1^3 \Omega_2}{\Omega_1^4 + \Omega_2^4} \tag{27b}$$

3.2 design procedure

The design process of the proposed 2DOF vibrational energy harvester consists of two steps. The first step is the vibration design. It starts from selecting the two target resonance frequencies Ω_1 and Ω_2. When the mass properties, i.e., m and J are given, the corresponding modes, i.e., vibration center, can be obtained from the design equations of Eqs. (22) and (23). The second step is the realization of the spring systems. The stiffness matrix can be synthesized from the calculated modes and target resonant frequencies. The spring properties, i.e., spring constant and locations of springs, can be found from the design equations of Eqs. (26) and (27). The flow chart for the design procedures is presented in Fig. 3.

Table 1 Input parameters for design of 2DOF vibrational energy harvester in a plane

Parameters	Value
Material of rigid body	Brass
Size of rigid body	$0.060(l) \times 0.014(w) \times 0.014(h)$ m^3
Size of device	$0.060(l) \times 0.060(w) \times 0.150(h)$ m^3
Mass of rigid body (m)	0.098 kg
Moment of inertia (J)	3.152×10^{-5} kg/m^2
Acceleration (a_{cc})	0.15 G
Target frequencies (Ω_1, Ω_2)	35, 38 Hz

4. Experimental study

4.1 Prototype design

When the target resonant frequencies are set to 35 and 38 Hz and the mass properties are given as Table 1, the *X*-coordinates of the vibration centers are calculated from Eqs. (22) and (23) to $x_1 = 0.0165$ and $x_2 = -0.0194$. The spring constant, k and location of springs are respectively obtained from Eqs. (26) and (27) as k = 1304.2 N/m, r_1 = 0.0163, and r_2 = 0.0192 m. The designed prototype of the harvester has been constructed and tested. Two coils are installed on front and rear side of a rigid body and connected in series. A pair of the plat type Halbach magnet array is mounted on the base platform as shown in Fig. 4. It

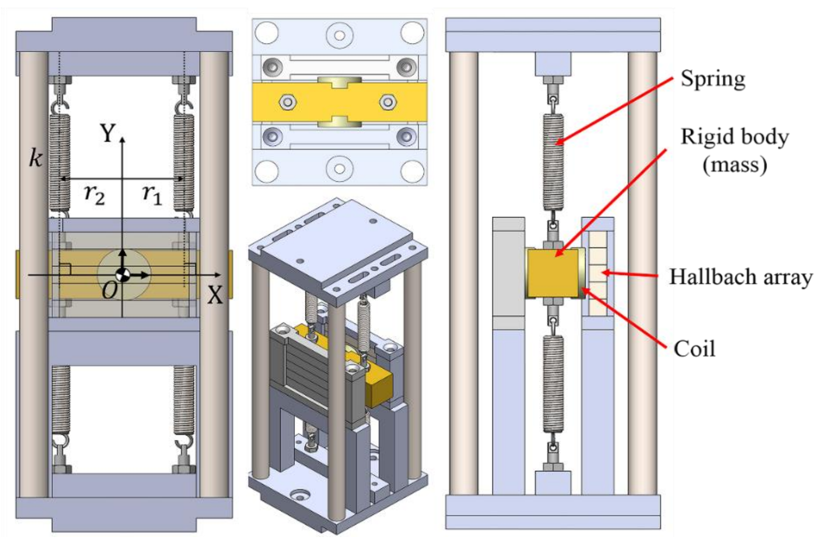

Fig. 4 Prototype of the 2DOF vibrational energy harvester

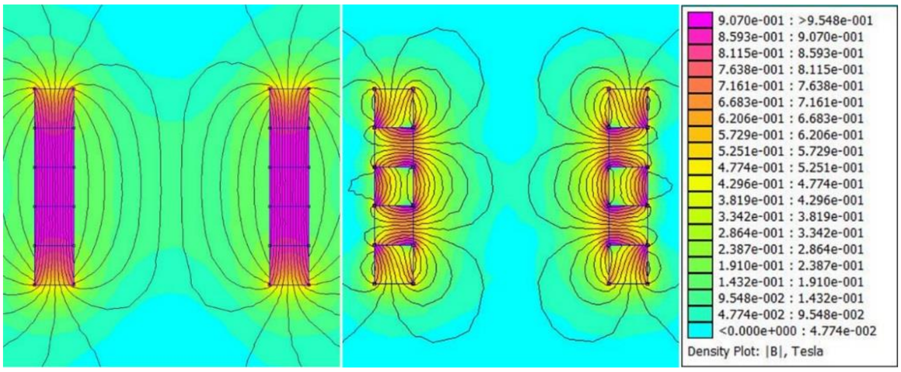

Fig. 5 Magnetic flux of normal (left) and Halbach (right) array pair by FEMM

Table 2 Physical parameters of electromagnetic transducer

Parameters	Value
Magnets	Neodymium magnets (5EA)
Size of magnet array	$0.060(l) \times 0.014(w) \times 0.014(h)$ m^3
Magnetic flux density	Max 8.06×10^{-1} T
Diameter of coil	1.500×10^{-2} m
Number of coil turn	1100
Internal resistance of coil	116.1 Ω

is suitable for the complex planar motion of the coil and provides a higher magnetic density than other architectures (Zhu *et al*. 2012). The maximum magnetic flux density was measured by gauss meter (Lutron GU3001) to 0.806 T, which is the twice of the value from the normal array. The FEMM simulation result in Fig. 5 compares the magnetic flux density distributions of two magnet array. It is clear that the magnetic flux density near the magnets of Halbach array is stronger than that of normal array. Both the measurement and the simulation show that the magnetic

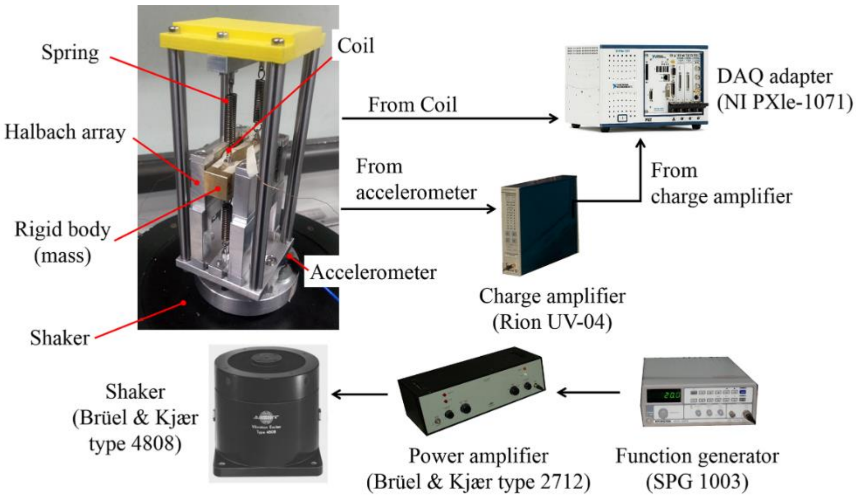

Fig. 6 Fabrication result and experimental setup of the 2DOF vibration harvester

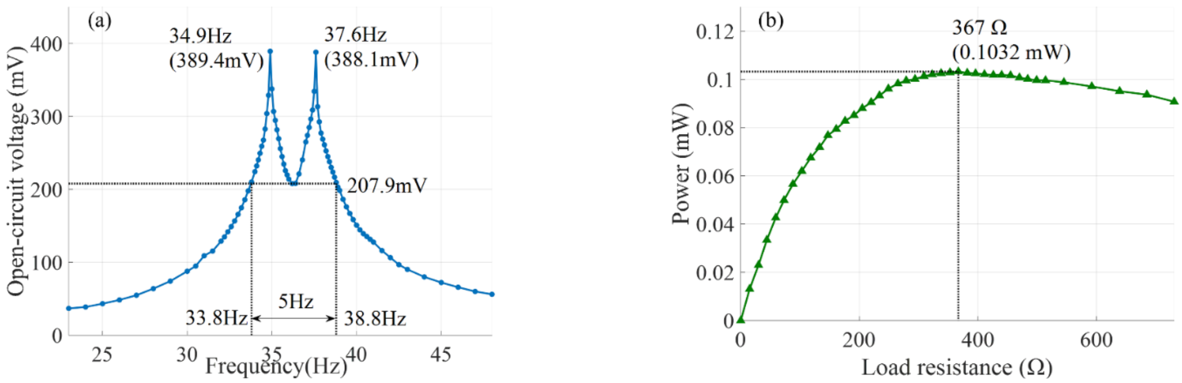

Fig. 7 (a) The total voltage output; and (b) optimal load resistance flux was improved when the Halbach array was utilized. The physical parameters of the proposed electromagnetic transducer are given in Table 2.

4.2 Experiment

Fig. 6 shows the experimental setup of the fabricated harvester. It is attached on the shaker, which provides the constant acceleration in the vertical direction. The output voltage from the electrical generator of the harvester is measured by the oscilloscope (National Instrument NI PXIe-1071). The experimental open-circuit voltage outputs from the acceleration input of 0.15 G (1.47 m/s^2) are shown in Fig. 7(a). They are well met with the designated target frequencies of 35 and 38 Hz, respectively. The proposed harvester can increase the bandwidth by connecting two peaks. The measured bandwidth is 5 Hz at the voltage level of 207.9 mV. The maximum output voltage of 389.4 mV is found at the first peak. Fig. 7(b) shows that the power output measured at 34.9 Hz when the load resistance is connected and changes from 0 to 700 Ω. The maximum output power is 0.1032 mW at 367 Ω, which can be expressed by the normalized power of 4.587 mW/G^2. It can also be normalized by both the volume and the acceleration level to 0.4143 kg s/m^3 (Beeby *et al*. 2007).

5. Conclusions

In this study, the design method of electromagnetic 2DOF vibration energy harvester is proposed. The vibration system is described via Plücker’s line coordinates. The design equations are obtained from the orthogonality of the modes and the identical work conditions. When the two target resonant frequencies and mass properties are specified, the locations for the vibration centers, stiffness constant, and spring positions can be obtained in the closed form. The numerical example and its realization are provided to verify the proposed method. The experiment shows that the measured resonant peaks are well met to the target frequencies and the bandwidth increases to 5 Hz at the voltage level of 207.9 mV. The normalized maximum output power is found to 4.587 mW/G^2.

Acknowledgments

This research was supported by the Academic Research fund of Hoseo University in 2015(2015-0120).

References

Ashraf, K., Md Khir, M.H., Dennis, J.O. and Baharudin, Z. (2013), “Improved energy harvesting from low frequency vibrations by resonance amplification at multiple frequencies”, *Sens. Actuators, A*, **195**, 123-132. https://doi.org/10.1016/j.sna.2013.03.026

Beeby, S.P., Torah, R.N., Tudor, M.J., Glynne-Jone P., O’Donnell T., Saha C.R. and Roy S. (2007), “A micro electromagnetic generator for vibration energy harvesting”, *J. Micromech. Microeng.*, **17**, 1257-1265. https://doi.org/10.1088/0960-1317/17/7/007

Blanchet, P. (1988), “Linear vibration analysis using screw theory”, Ph.D. Dissertation; Georgia Institute of Technology, Atlanta, GA, USA.

Chen, S.-J. and Wu, J.-Y. (2016), “Fabrication of a 2-DOF electromagnetic energy harvester with in-phase vibrational bandwidth broadening”, *Smart Mater. Struct.*, **25**, 095047. https://doi.org/10.1088/0964-1726/25/9/095047

Ferrari, M., Ferrari, V., Guizzetti, M., Marioli, D. and Taroni, A. (2008), “Piezoelectric multifrequency energy converter for power harvesting in autonomous microsystems”, *Sens. Actuators, A*, **142**, 329-335. https://doi.org/10.1016/j.sna.2007.07.004

Griffis, M. and Duffy, J. (1991), “Kinestatic control: a novel theory for simultaneously regulating force and displacement”, *J. Mech. Des.*, **113**, 508-515. https://doi.org/10.1115/1.2912812

Jang, S.-J., Rustighi, E., Brennan, M.J, Lee, Y.P. and Jung, H.-J. (2010), “Design of a 2DOF vibrational energy harvesting device”, *J. Intell. Mater. Syst. Struct.*, **22**, 443-448. https://doi.org/10.1177/1045389X10393766

Kim, I.-H., Jung, H.-J., Lee, B.M. and Jang, S.-J. (2011), “Broadband energy-harvesting using a two degree-of-freedom vibration body”, *Appl. Phys. Lett.*, **98**, 214102. https://doi.org/10.1063/1.3595278

Kim, J.-M., Han, M., Lim, H.J., Yang, S. and Sohn, H. (2016), “Operation of battery-less and wireless sensor using magnetic resonance based wireless power transfer through concrete”, *Smart Struct. Syst., Int. J.*, **17**(4), 631-646. https://doi.org/10.12989/sss.2016.17.4.631

Liu, H., Soon, B.W., Wang, N., Tay, C.J., Quan, C. and Lee, C. (2012), “Feasibility study of a 3D vibration-driven electromagnetic MEMS energy harvester with multiple vibration modes”, *J. Micromech. Microeng.*, **22**, 125020. https://doi.org/10.1088/0960-1317/22/12/125020

Makihara, K., Hirai, H. and Yamamoto, Y. (2015), “Self-reliant wireless health monitoring based on tuned-mass-damper mechanism”, *Smart Struct. Syst., Int. J.*, **15**(6), 1625-1642. https://doi.org/10.12989/sss.2015.15.6.1625

Marin, A., Turner, J., Ha, D.S. and Priya, S. (2013), “Broadband electromagnetic vibration energy harvesting system for powering wireless sensor nodes”, *Smart Mater. Struct.*, **22**, 075008. https://doi.org/10.1088/0964-1726/22/7/075008

Meirovitch, L. (2001), *Fundamentals of Vibration*, McGraw-Hill Companies, Inc., New York, NY, USA.

Nammari, A., Caskey, L., Negrete, J. and Bardaweel, H. (2018), “Fabrication and characterization of non-resonant magneto-mechanical low-freqeucny vibration energy harvester”, *Mech. Syst. Sig. Process.*, **86**, 29-39. https://doi.org/10.1016/j.ymssp.2017.09.036

Nico, V., Boco, E., Frizzell, R. and Punch, J. (2016), “A high figure of merit vibrational energy harvester for low frequency applications”, *Appl. Phys. Lett.*, **108**, 013902. https://doi.org/10.1063/1.4939545

Marian, L. and Giaralis, A. (2017), “The tuned mass-damper-inerter for harmonic vibrations suppression, attached mass reduction, and energy harvesting”, *Smart Struct. Syst., Int. J.*, **19**(6), 665-678. https://doi.org/10.12989/sss.2017.19.6.665

O’Donoghue, D., Frizzell, R. and Punch, J. (2018), “Scaling and characterisation of a 2-DoF velocity amplified electromagnetic vibration energy harvester”, *Smart Mater. Struct.*, **27**, 075019. https://doi.org/10.1088/1361-665X/aac297

Ramlan, R., Brennan, M.J., Mace, B.R. and Kovacic, I. (2010), “Potential benefits of a non-linear stiffness in an energy harvesting device”, *Nonlinear Dyn.*, **59**, 545-558. https://doi.org/10.1007/s11071-009-9561-5

Shahruz, S.M. (2006), “Design of mechanical band-pass filters with large frequency bands for energy scavenging", *Mechatronics*, **16**, 523-531. https://doi.org/10.1016/j.mechatronics.2006.04.003

Tang, L. and Yang, Y. (2012), "A nonlinear piezoelectric energy harvester with magnetic oscillator", *Appl. Phys. Lett.*, **101**, 094102. https://doi.org/10.1063/1.4748794

Wang, H. and Tang, L. (2017), "Modeling and experiment of bistable two-degree-of-freedom energy harvester with magnetic coupling", *Mech. Syst. Sig. Process*, **86**, 29-39. https://doi.org/10.1016/j.ymssp.2016.10.001

Wong, Z.J., Yan, J., Soga, K. and Seshia, A. (2009) "A multi-degree-of-freedom electrostatic MEMS power harvester", *Power Micro Electro Mechanical Systems*, Washington, DC, USA, December.

Wu, H., Tang, L., Yang, Y. and Soh, C.K. (2014), "Development of a broadband nonlinear two degree-of-freedom piezoelectric energy harvester", *J. Intell. Mater. Syst. Struct.*, **25**, 1875-1889. https://doi.org/10.1177/1045389X14541494

Zhang, Y., Wang, T., Zhang, A., Peng, Z., Luo, D., Chen, R. and Wang, F. (2016), "Electrostatic energy harvesting device with dual resonant structure for wideband random vibration sources at low frequency", *Rev. Sci. Instrum.*, **87**, 125001. https://doi.org/10.1063/1.4968811

Zhu, D., Tudor, M.J. and Beeby, S.P. (2010), "Strategy for increasing the operating frequency range of vibration energy harvesters: a review", *Meas. Sci. Technol.*, **21**, 022001. https://doi.org/10.1088/0957-0233/21/2/022001

Zhu, D., Beeby, S., Tudor, J. and Harris, N. (2012), "Vibration energy harvesting using the Halbach array", *Smart Mater. Struct.*, **21**, 075020. https://doi.org/10.1088/0964-1726/21/7/075020

HJ